Energy Transfer Upconversion Processes

Seth D. Melgaard
NLO Final Project

1. Up-conversion Processes

The usual fluorescence behavior follows Stokes law, where exciting photons are of higher energy than emitted photons. Anti-Stokes processes usually concern emitted energies in excess of excited energies by only a few kT. These processes include anti-Stokes emission by the thermal bands or by the Raman effect. There are processes, however, in which emission photon energy exceeds excited photon energy by 10 - 100 kT. This includes energy transfer upconversion (APTE or ETU), multi-step excitations from excited state absorption (ESA), cooperative upconversion, and the photon avalanche effect. These upconversion processes are compared with the relative efficiencies for second harmonic generation (SHG) and 2-photon absorption (TPA) in Fig. 1.

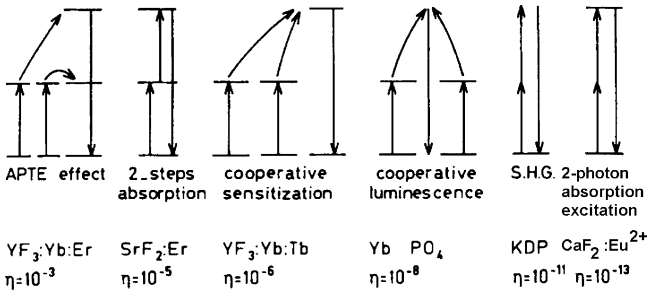

Fig. 1. Two photon upconversion processes with relative efficiencies [1].

ETU is seen in various types of ion-doped solids such as crystals or glasses, most notably in laser crystals. ETU is often an unwanted effect when building a laser since it is a form of non-radiative decay which is an inefficiency leading to unwanted heat in the laser crystal, wasting energy. Like most phenomena, ETU is not all bad. For example it can be used to create an up-converted room temperature CW laser when pumping Thulium at 1120-1140nm and generating a blue laser at 480nm [12-14].

2. The basics of ETU

Energy transfer upconversion (ETU) is the result of successive energy transfers between ions at different sites. Since the ETU process involves the mutual interaction between ions, it is required that the concentration of ions is sufficient to allow energy migration between ions, however it does not require charge transport. The first ion to be excited is called a sensitizer (S) and the ion to which energy is transferred is called the activator (A). In literature, the two ions are sometimes called donor and acceptor, respectively, but since this can be confused with semiconductors, sensitizer and activator are preferred.

There are three types of distinguished energy transfer depicted in Fig. 2, radiative (a), nonradiative (b), and phonon-assisted (c).

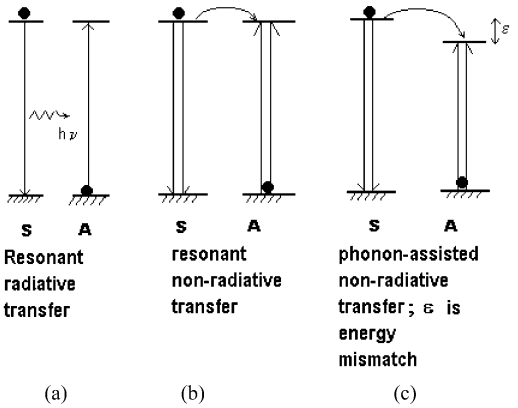

Figure 2. Three types of energy transfer. Successive energy transfers lead to upconversion [1].

(a) Radiative energy transfer occurs when a photon is emitted by the sensitizer and absorbed by the activator, and hence is dependent on the sample shape. Longer dimensions allow for a greater possibility for absorption by the activator. Depending on the degree of overlap between the emission spectra of S and the absorption spectra of A, the shape of the sensitizer emission will change according to the activator concentration. This means radiative and nonradiative energy transfer can be distinguished by looking at reabsorption effects. The probability for an energy transfer to occur as a function of distance R is given by [1],

$$P_{SA}(R) = \frac{\sigma}{4\pi R^2 \tau_S} \int g_S(\nu) g_A(\nu) d\nu \qquad (1)$$

where t_S is the sensitizer lifetime, σ_A is the absorption cross section, and the integral is the spectral overlap between S and A. The R^{-2} distance dependence between ions helps determine concentration levels, as well as determining the host based on interatomic distances.

(b) Nonradiative energy transfer is an interaction that occurs between two ions with nearly equal energy between the ground state and an excited state. Given enough ion interaction, the excitation will jump from one ion to another. The probability for energy transfer goes as,

$$P_{SA} = \frac{(R_0/R)^n}{\tau_S} \qquad (2)$$

where τ_S is the sensitizer lifetime and R_0 is the critical transfer distance for which excitation transfer and spontaneous deactivation of the sensitizer have equal probability. The exponent, n, is an integer that goes as

n = 6 for dipole-dipole interactions
n = 8 for dipole-quadrupole interactions
n = 10 for quadrupole-quadrupole interactions

(c) A phonon-assisted energy transfer occurs between two ions with different energy separations. The probability for energy transfer should go to zero as the energy integral overlap goes to zero (Eqn. 1), however it can still take place for small energies (~.01 eV) provided energy is conserved through production and annihilation of a few phonons. In rare-earth ions, however, energies differences an order of magnitude higher are possible and so multi-phonon processes must be considered.

Because both the quantum mechanical treatment [1-5] and the macroscopic treatment [6-9] of the energy transfer process are lengthy and cumbersome, it is more instructive to point out some of the expected behavior such as the power dependence.

Pollnau et al. have shown the power dependence starting from rate equations for ETU in an ion containing four excited state levels (appropriate for Er^{3+}) with population N_i and corresponding parameters W_i [10],

$$N_0 \approx const., \tag{3}$$

$$dN_1/dt = \rho_p \sigma_0 N_0 - 2W_1 N_1 N_1 - W_2 N_1 N_2 - W_3 N_1 N_3 - A_1 N_1 + \beta A_2 N_2, \tag{4}$$

$$dN_2/dt = W_1 N_1 N_1 - W_2 N_1 N_2 - A_2 N_2 + \beta_3 A_3 N_3, \tag{5}$$

$$dN_3/dt = W_2 N_1 N_2 - W_3 N_1 N_3 - A_3 N_3 + \beta_4 A_4 N_4, \tag{6}$$

$$dN_4/dt = W_3 N_1 N_3 - A_4 N_4. \tag{7}$$

Solutions to the rate equations exist [10] for small upconversion (1) and large upconversion (2), and are summarized in Table 1.

(1) Small upconversion:

For (i) $\beta_i = 1$ and (ii) $\beta_i = 0$, steady-state solutions are,

$$N_i = A_1^{-i} \prod_{j=2,\ldots,i} [W_{j-1} A_j^{-1}] (\rho_p \sigma_0 N_0)^i \qquad i = 1,\ldots,n. \tag{8}$$

(2) Large upconversion:

For (i) $\beta_i = 1$, steady-state solutions are,

$$N_i = \prod_{j=2,\ldots,i} [W_{j-1} A_j^{-1}] \prod_{k=2,\ldots,n-1} [A_k^{i/n}] \times \prod_{l=1,\ldots,n-1} [W_l^{-i/n}] (\rho_p \sigma_0 N_0)^{i/n} \qquad i = 1,\ldots,n. \tag{9}$$

For (i) $\beta_i = 0$,

$$N_i = 0.5 W_1^{0.5} W_i^{-1} (\rho_p \sigma_0 N_0)^{0.5} \qquad i = 1,\ldots,n. \tag{9}$$

$$N_n = 0.25 A_n^{-1} \rho_p \sigma_0 N_0 \tag{10}$$

Influence of upconversion	Upconversion mechanism	Predominant decay route	Fraction of absorbed pump power	Power dependence	From level
(1) Small	ETU or ESA	next lower state or ground state	small or large	$N_i \sim P^i$	$i = 1, \ldots, n$
(2) Large	(A) ETU	(i) next lower state	small or large	$N_i \sim P^{i/n}$	$i = 1, \ldots, n$
		(ii) ground state	small or large	$N_i \sim P^{1/2}$	$i = 1, \ldots, n-1$
				$N_i \sim P^1$	$i = n$
	(B) ESA	(i) next lower state	(a) small	$N_i \sim P^i$	$i = 1, \ldots, n$
			(b) large	$N_i \sim P^{i/n}$	$i = 1, \ldots, n$
		(ii) ground state	small or large	$N_i \sim P^0$	$i = 1, \ldots, n-1$
				$N_i \sim P^1$	$i = n$

TABLE I. Characteristic slopes of the steady-state excited-state population densities N_i of levels $i = 1 \ldots n$ and luminescences from these states for *n-photon* excitation. The investigated limits are: (1) small upconversion or (2) large upconversion by (A) ETU or (B) ESA, decay predominantly (i) into the next lower-lying state or (ii) by luminescence to the ground state, and (a) a small or (b) a large fraction of pump power absorbed in the crystal [10].

The high efficiency of ETU (given optimal atomic seperation) comes at the cost of a long fluorescence lifetime, Fig. 3. Termed phosphorescence, the long lifetime is due to the transfer of energy into 'forbidden' states and because of this slowness, it is susceptible to other forms of non-radiative decay. In order to effectively generate

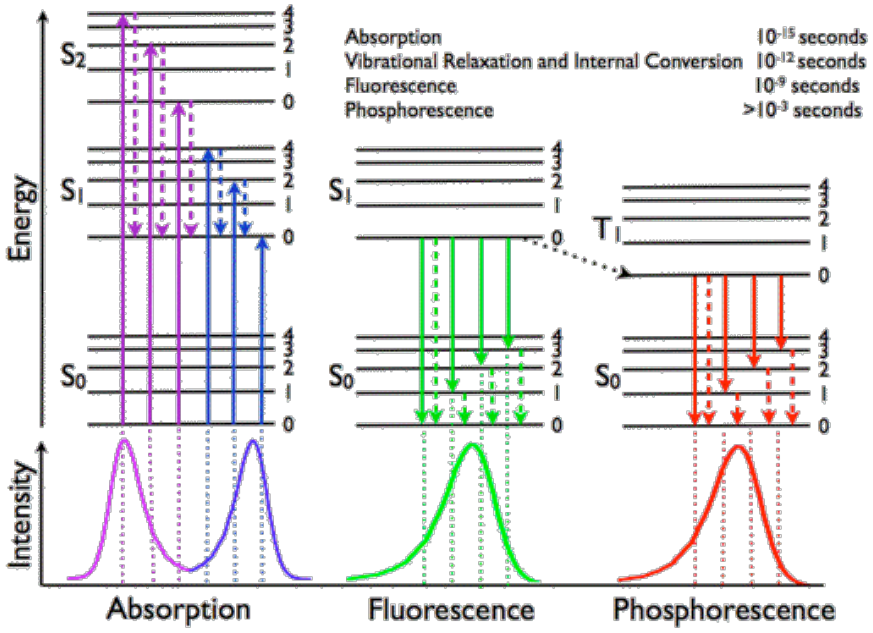

Figure 3. Relative time scales for absorption, fluorescence and phosphorescence.

phosphorescence, host materials with low phonon energies and minimal impurities is desired.

3. Applications for ETU

Because the efficiency for ETU is high, a number of uses for conversion of IR to visible light are possible. This process can be useful for IR detection and ETU pumped lasers. Something useful for anyone who works with IR lasers is an IR detection card. The 1.5μm cards use polycrystalline Er^{3+} phosphors [11] that follow the ETU scheme shown in Fig. 4, and allow a simple method for detecting otherwise invisible light.

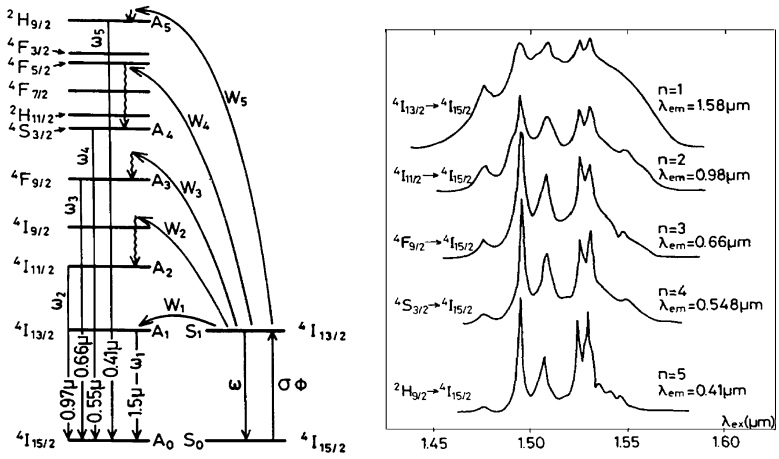

Figure 4. (left) Er^{3+} ETU levels. (right) Corresponding fluorescence spectra.

Perhaps the most interesting application is ETU pumped lasers. These can be single ion RE doped systems, or co-doped with one RE ion as the sensitizer and another the activator. Initial attempts at CW ETU pumped lasers required cooling crystals to very low temperatures making them impractical. More recently, a room temperature, 3mm long single crystal 3%Yb-1%Er:YLF crystal pumping the high Yb absorption at 960nm with 1.6W reached a useful output of 40mW at 551nm with a threshold of 418 mW [15].

Glass fibers allow for high pumping density over long lengths. Fluoride fibers in particular favor anti-Stokes laser because of long-lived metastable states with low energy phonons and easily achieved ground state saturation. The first room temperature CW fiber laser used Ho^{3+} doped fluoride fiber [16]. Er^{3+} doped glass fibers have generated three level laser emission at 540nm pumped at 801nm. So far only two-photon processes have been mentioned, but a Tm^{3+} doped ZBLAN fiber has demonstrated a three-photon upconversion laser when pumped with 1.12μm and emitting at 480nm with a threshold of 30mW [17]. A final example is one of Pr3+-doped fluoride fibers. Because of their low phonon energy with respect to Pr^{3+} emitting level energy differences, CW room-temperature anti-Stokes lasers at blue, green, and red wavelengths in a single fiber have been demonstrated [18].

4. References

[1] Francois Auzel. Upconversion and Anti-Stokes Processes with f and d Ions in Solids. Chem. Rev. 104: 139-173, Nov. 2003.
[2] Forster, T. *Ann. Phys.* **1948,** *2,* 55.
[3] Dexter, D. L. *J. Chem. Phys.* **1953,** *21,* 836.
[4] Kushida, T. *J. Phys. Soc. Jpn.* **1973,** *34,* 1318.
[5] Pouradier, J. F.; Auzel, F. *J. Phys. (France)* **1978,** *39,* 825.
[6] Axe, J. D.; Weller, P. F. *J. Chem. Phys.* **1964,** *40,* 3066.
[7] Orbach, R. *Optical Properties of Ions in Solids;* DiBartolo, B., Ed.; Plenum Press: New York, 1975; p 445.(32)
[8] Miyakawa, T.; Dexter, D. L. *Phys. Rev.* **1971,** *B1,* 70.
[9] Weber, M. J. *Phys. Rev.* **1971,** *B4,* 2932.
[10] Pollnau, M.; Gamelin, D. R. Luthi, S. R.; Gudel, H.; Hehlen, M. P. *Phys. Rev.* **2000,** *61,* 5.
[11] *Photo-Turkey-1;* Sumita Optical Glass Inc. (4-7-25 Harigaya, Urawa-City, Saitama, Japan), 1994.
[12] S. G. Grubb *et al.*, "CW room-temperature blue upconversion fibre laser", Electron. Lett. 28, 1243 (1992)
[13] R. Paschotta *et al.*, "Characterization and modeling of thulium:ZBLAN blue upconversion fiber lasers", J. Opt. Soc. Am. B 14 (5), 1213 (1997)
[14] R. Paschotta *et al.*, "230 mW of blue light from a Tm-doped upconversion fibre laser", IEEE J. Sel. Top. Quantum Electron. 3 (4), 1100 (1997)
[15] Heine, F.; Heumann, E; Danger, T.; Schweizer, T.; Huber, G. *Appl. Phys. Lett.* **1994,** *65,* 383.
[16] Allain, J.-Y.; Monerie, M.; Poignant, H. *Electron. Lett.* **1990,** *26,* 261.
[17] Grubb, S. G.; Bennett, K. W.; Cannon, R. S.; Humer, W. F. *Electron. Lett.* **1992,** *28,* 1243.
[18] Smart, R. G.; Hanna, D. C.; Tropper, A. C.; Davey, S. T.; Carter, S. F.; Szebesta, D. *Electron. Lett.* **1991,** *27,* 1308.